ELSEVIER

Catalysis Today 55 (2000) 103–116

CATALYSIS TODAY

www.elsevier.com/locate/cattod

Mg- and Ni-containing layered double hydroxides as soda substitutes in the aldol condensation of acetone

Federica Prinetto [a,1], Didier Tichit [a,*], Remi Teissier [b], Bernard Coq [a]

[a] *UMR 5618 CNRS-ENSCM, 8 rue Ecole Normale, 34296 Montpellier Cedex 5, France*
[b] *ELF-Atochem CRRA, rue H. Moissan, BP63 69310 Pierre-Benite, France*

Abstract

A series of layered double hydroxides (LDHs) containing Mg^{2+} or Ni^{2+} as divalent and Al^{3+} or Ga^{3+} as trivalent cations were used as catalysts in order to substitute NaOH in the selective condensation of acetone into diacetonealcohol. With this aim the LDHs were totally exchanged with OH^- anions and acquired the meixnerite-like structure, showing a high concentration of active basic sites. These meixnerite-like structures were prepared by reconstruction under appropriate conditions of the mixed oxides obtained by calcination. The complete reconstruction was easily achieved in water at ambient temperature and pressure for Mg-containing samples, while more severe conditions were needed for the Ni-containing one, as shown by XRD, TEM and UV–VIS DR spectroscopy. The reconstruction degree of Ni/Al mixed oxides was markedly improved by hydrothermal treatments under ammonia. The nature of the cations influenced the acid–base properties of the mixed oxides, as evidenced by NH_3 and CO_2 TPD experiments, and consequently their catalytic activities. The catalytic activities of the meixnerite-like forms were related both to the basicity of the corresponding mixed oxide and to the reconstruction degree in the lamellar form, thus to the density of the OH^- sites. Indeed, the loss of the lamellar structure was the main cause of the catalyst deactivation. ©2000 Elsevier Science B.V. All rights reserved.

Keywords: Aldol condensation; Acetone; Basic solids; Layered double hydroxides; Meixnerite-like compounds

1. Introduction

Aldol condensation of acetone using NaOH or KOH as catalysts is the industrial route for the production of diacetonealcohol [1]. This reaction is slightly exothermic, therefore advantageously performed at low temperature, the thermodynamic equilibrium reaching 23% conversion at 273 K [2].

The substitution of liquid bases with basic solid catalysts is particularly suitable to reduce the environmental impact of the process, avoiding for example the use of consistent amounts of phosphoric acid to neutralize the catalyst and the subsequent production of salts. Layered double hydroxides (LDHs) are a class of basic solids showing very attractive properties, particularly for the condensation reactions [3]. LDHs are represented by the general formula $[M_{1-x}{}^{2+}\ M_x{}^{3+}\ (OH)_2]^{x+}\ A_{x/z}{}^{z-}\cdot mH_2O(M^{2+} = Mg^{2+}, Ni^{2+}, Zn^{2+}, \ldots;\ M^{3+} = Al^{3+}, Fe^{3+}, Ga^{3+}, \ldots;\ A^{z-} = CO_3{}^{2-}, NO_3{}^{-}, Cl^{-}, \ldots)$. Their structure consists of brucite-type layers, where the substitution of M^{2+} with M^{3+} cations results into a net positive charge, compensated by interlayer anions [4–6]. The

---

[*] Corresponding author. Tel.: +33-467-144-322; fax: +33-467-144-349
E-mail address: tichit@cit.enscm.fr (D. Tichit)
[1] Present address: Dipartimento di Chimica IFM, Università di Torino, Via P. Giuria 7, 10125 Torino, Italy.

PII: S0920-5861(99)00230-8

meixnerite-like form of Mg/Al-LDHs, which corresponds to the lamellar structure totally exchanged by OH^- anions [7–9], possesses high Brønsted basicity, and therefore high activity in the aldol condensation reactions, where OH^- sites are required [9–11], as is the case for the selective obtention of diacetonealcohol from acetone [12,13]. However, the direct anionic exchange of the hydrotalcite by OH^- anions is not efficient due to the high affinity of these materials for carbonate anions [14] or to the impossibility to perform treatments with strong alkaline solutions without inducing concurrent dissolution of the solids. Another route, frequently used for the preparation of the meixnerite [15] and extended to the intercalation of aromatic molecular anions [16] or voluminous organic species [17], consists to dehydroxylate the layers and to eliminate the vaporizable anions by thermal treatment of the LDHs which concurrently moves to the mixed oxide structure. The latter is then reconstructed into the LDH structure by rehydroxylation in an aqueous solution containing the anionic species to intercalate, using its so-called memory effect [18]. Following this process, the catalytically active meixnerite structure is achieved by thermal decomposition of the precursor Mg/Al-LDH at a temperature in the range of 673–873 K and subsequent reconstruction in water of the lamellar structure with the unique OH^- compensating anions.

We have tried to extend this procedure to LDH structures containing other divalent and trivalent cations than Mg^{2+} and Al^{3+}, able to modify their catalytic properties, and particularly to Ni/Al-LDH. These compounds, corresponding to the natural mineral takovite [4,14], are easily obtained in a well crystallized form in laboratory. As previously reported [19], the Ni-based layered structures have higher thermal and chemical stabilities than the Mg-ones. This can be advantageously used for regenerating the catalysts through processes involving calcination steps. In contrast, the Ni-containing mixed oxides present a lower ability toward reconstruction into the LDH form than the Mg-containing ones [20]. Our aim was, therefore, to optimize the reconstruction of the Ni-LDHs in the meixnerite-like form and to compare their catalytic activity to that of the parent Mg/Al compounds.

Furthermore, well crystallized LDH structure containing Ga^{3+} as trivalent cation have been claimed to exist in a large range of Mg^{2+}/Ga^{3+} ratios [21–23], showing exceptional basic properties [22]. This was an incitement to investigate the performances of Ga-containing LDHs.

One of the main goal was to define LDHs structures and activation procedures making catalysts able to replace NaOH for clean processes.

2. Experimentals

2.1. Sample preparation

Samples were prepared by co-precipitation at constant pH in the range 9–11 [4,6] of adequate amounts of 0.9 M M^{2+} (Mg^{2+} or Ni^{2+}) and 0.18–0.3 M M^{3+} (Al^{3+} or Ga^{3+}) nitrate salt solutions with 1.5 M NaOH or 1.5 M NaOH + 2×10^{-2} M Na_2CO_3 solution. The precipitated gels were then hydrothermally treated in the mother liquor at 353 K for 17 h, repeatedly washed into deionized water (Na < 100 ppm) and dried at 353 K (samples denominated as prepared, a.p.)

The samples will be hereafter referred to as $M^{2+} M_x{}^{3+}$, where M^{2+} and M^{3+} are the divalent and trivalent cations involved, respectively, and x is their atomic ratio determined in the solid.

2.2. Catalyst activation and catalytic tests

The activation of the LDHs into the meixnerite-like forms was performed in two steps, including calcination and rehydroxylation. The a.p. samples were calcined at temperatures in the range 633–823 K into a N_2/O_2 flow of about 100 ml min^{-1}. The heating rate was 1 K min^{-1} and the final temperature was maintained for 6 h. Different rehydroxylation procedures were then adopted according to the M^{2+} involved: (i) calcined Mg-LDH powders were dispersed under vigorous magnetic stirring during 1 h into decarbonated water at 298 K and 1×10^5 Pa; (ii) calcined Ni-LDH powders were treated in decarbonated water into a 120 ml autoclave at temperatures ranging from 298 to 433 K, under autogene pressure (1×10^5–6×10^5 Pa) during increasing times up to 120 h. Experiments were also performed in the same temperature and pressure conditions into NH_4OH 1 wt.% aqueous solution. For sake of brevity, the most frequently used rehydroxylation treatment during 120 h at 433 K and

6×10^5 Pa will be hereafter referred to as standard rehydroxylation treatment (s.r.t.). Remaining water after the rehydroxylation step was eliminated by repeatedly washing of the sample with acetone.

Aldol condensation of acetone was performed in an ice bath at 273 K in a well agitated 100 ml round bottom flask under N_2 atmosphere. For catalytic tests, 1.5 g of solid were used, the catalyst on acetone ratio being 4.7 wt.%. Acetone (from Aldrich, >99.9%) was previously purified using a 3X molecular sieve, activated at 523 K. The reaction mixture was analyzed by gas chromatography using an OV1 column. Only diacetonealcohol (DAA) and mesityl oxide (MO) were obtained as reaction products. DAA conversion ((mol DAA formed × 2/initial mol acetone) × 100) is reported as a function of contact time.

2.3. Sample characterization

Chemical analyses of the solids were performed at the Service Central d'Analyse du CNRS (Solaize, France).

The XRD powder patterns were collected on a CGR Theta 60 instrument using monochromatized Cu Kα1 radiation ($\lambda = 1.542$ Å, 40 kV and 50 mA). BET specific surface areas were determined by N_2 adsorption at 77 K on a Micromeritics ASAP 2100 on the calcined samples, previously outgassed at 523 K (10^{-4} Pa).

Thermogravimetric analyses (TG) were carried out on a Setaram TG 85 1000°C microbalance operating in a flow of dry nitrogen (110 ml min^{-1}) at a heating rate of 2 K min^{-1} from 298 to 1023 K on 20 mg of sample.

Transmission electron microscopies and high resolution transmission electron microscopies (TEM and HRTEM) were performed with a Jeol Jem 2000 microscope, equipped with a top entry stage.

UV–VIS Diffuse Reflectance (UV–VIS DR) spectra were recorded on a Perkin–Elmer Lambda 16 spectrometer, equipped with an integration sphere. Data were displayed as $F(R_\infty)$ vs. wavenumbers, being $F(R_\infty)$ the Kubelka–Munk function: $F(R_\infty) = (R_\infty - 1)^2/2R_\infty$, where R_∞ is the diffuse reflectance of the sample considered of infinite thickness. Total basicity of the mixed oxides was measured by thermal adsorption and desorption of CO_2 with a Setaram DSC-111 microcalorimeter. The samples were previously outgassed at 723 K, cooled to 373 K and contacted with flowing CO_2. The thermal event in the microcalorimetric cell was recorded. After purging the physisorbed CO_2 under He flow, the temperature programmed desorption (TPD) of CO_2 was performed under He flow from 373 to 723 K (heating rate 10 K min^{-1}).

Total acidity was measured by TPD of NH_3 using a conductivity cell for the detection of the effluent gases. The samples were previously outgassed at 723 K, cooled to 373 K and contacted with NH_3 vapor. After purging, the temperature was increased up to 723 K (heating rate 10 K min^{-1}) and evolved ammonia was trapped in a HCl solution and finally titrated.

3. Results and discussion

3.1. Chemical and XRD characterizations

3.1.1. As prepared samples

The precipitation pH adopted for sample preparation (Table 1) was chosen in order to obtain a quantitative precipitation yield of the LDHs. The M^{2+}/M^{3+} ratios found in the solids were almost coincident with those adopted in the solutions for Al-containing samples. In contrast, in the case of Ga-LDHs, we noted a marked increase of the M^{2+}/M^{3+} ratio, when passing from the solution to the solid, according to the high solubility of gallium hydroxide into alkaline media [21]. In agreement, the discrepancy between the M^{2+}/M^{3+} ratio in the solid and in the solution was larger in MgGa4.53 than in MgGa3.61, the first being prepared at higher pH. For all the a.p. samples, the XRD patterns were characteristics of well crystallized LDH structures (Fig. 1). The nature of the divalent cation had a negligible influence on the crystallinity, as seen comparing the patterns of Mg- and Ni-containing LDHs. In contrast, the substitution of Al^{3+} with Ga^{3+} induced an increase of the crystallinity, possibly due to an increase of the ordering in the LDH structure. However, weak amounts of brucite and probably of an amorphous Ga phase could be detected on MgGa6.94 and MgGa3.61, respectively. The higher M^{2+}/M^{3+} ratios found on Mg/Ga LDHs were normally indicative of a lower electropositive layer charge than on Mg/Al ones, prepared in the

Table 1
Synthesis parameters, chemical composition and morphologic features of LDH-samples

Sample	pH	M^{2+}/M^{3+} solution	M^{2+}/M^{3+} solid	Chemical composition[a]	d_{003} (Å)
MgAl2.69	9.0	3	2.69	$Mg_{0.729}$ $Al_{0.271}$ $(OH)_2$ $(CO_3)_{0.024}$ $(NO_3)_{0.223}\cdot0.48$ H_2O	8.74
MgAl2.89	10.5	3	2.89	$Mg_{0.743}$ $Al_{0.257}$ $(OH)_2$ $(CO_3)_{0.106}$ $(NO_3)_{0.207}\cdot0.46$ H_2O	8.47
MgGa3.61	9.0	3	3.61	$Mg_{0.783}$ $Ga_{0.217}$ $(OH)_2$ $(CO_3)_{0.032}$ $(NO_3)_{0.176}\cdot0.58$ H_2O	8.07
MgGa4.53	10.5	3	4.53	$Mg_{0.819}$ $Ga_{0.181}$ $(OH)_2$ $(CO_3)_{0.142}$ $(NO_3)_{0.021}\cdot0.52$ H_2O	8.04
MgGa6.94	11.0	5	6.94	$Mg_{0.874}$ $Ga_{0.126}$ $(OH)_2$ $(CO_3)_{0.403}$ $(NO_3)_{0.010}\cdot0.64$ H_2O	8.05
NiAl2.98	9.0	3	2.98	$Ni_{0.749}$ $Al_{0.251}$ $(OH)_2$ $(CO_3)_{0.093}$ $(NO_3)_{0.032}\cdot0.51$ H_2O	8.34

[a] Water content was determined from thermo-gravimetric analysis.

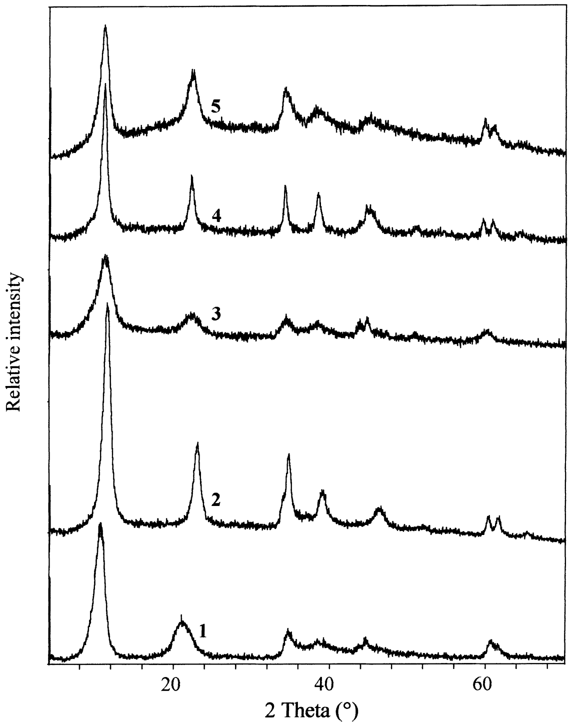

Fig. 1. XRD spectra of a.p. LDHs. MgAl2.89, (curve 1); NiAl2.98, (curve 2); MgGa6.94, (curve 3); MgGa4.53, (curve 4); MgGa3.61, (curve 5).

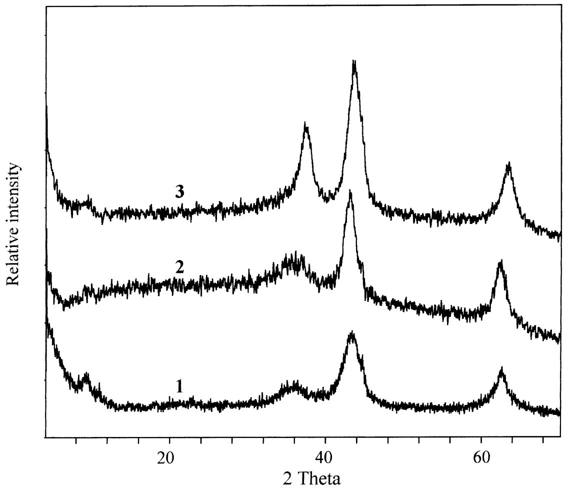

Fig. 2. XRD spectra of LDHs calcined at 723 K. MgAl2.89, (curve 1); NiAl2.98, (curve 2); MgGa3.61, (curve 3).

same conditions. Therefore, higher interlayer distances were expected on Ga-LDHs, since they are determined by the electrostatic interaction between the brucite-like layer and the anions. Furthermore, Ga^{3+} ions are expected to have a lower polarizing power, since their ionic radius (0.062 nm) is larger than that of Al^{3+} (0.050 nm) [24]. In contrast, smaller interlayer distances were obtained from the position of the (0 0 3) reflections in the XRD patterns on all the Ga-containing samples (Table 1). This reinforced the hypothesis of the presence of small amounts of amorphous Ga-containing ones among the additional phases detected by XRD, although pure LDH phases are claimed to exist in a very wide Mg^{2+}/Ga^{3+} range [21,22].

3.1.2. Calcined samples

The calcination at 633–823 K of the different a.p. samples, performed in order to decompose the interlayer anions, led to the complete disappearance of the XRD patterns of the LDH structure and to the appearance of the characteristic patterns of mixed oxides of MgO [11,20] or NiO type [20,25–27]. Fig. 2 shows the XRD patterns after calcination at 723 K of MgAl2.89, MgGa3.61 and NiAl2.98 with rather similar M^{2+}/M^{3+} ratios. As expected, the crystallographic parameters of the Mg(Al)O mixed oxide obtained from MgAl2.89 were slightly lower than in pure MgO (periclase, JCPDS file n. 43-1022), due to the smaller ionic radius of Al^{3+} than Mg^{2+} [24]. According to the literature [20], an additional weak reflection at $d = 0.25$ nm is assigned either to a magnesium aluminate-type phase or to the location of Mg^{2+} or M^{3+} cations on tetrahedral interstitial sites in the MgO lattice. The non-horizontal baseline observed in the XRD pattern of the Mg(Ga)O mixed oxide obtained from MgGa3.61 could account for the presence of an amorphous Ga_2O_3 phase. No reflections due to a spinel-like phase were detected, although its formation on Mg/Ga-LDHs had been revealed after calcination at quite low temperature (773 K) [20].

Analogously to Mg-containing samples, the crystallographic parameters of the Ni(Al)O mixed oxide obtained from NiAl2.98 were shifted toward lower values in comparison to pure NiO with rhombohedric structure (JCPDS file n. 22-1189). A model accounting for the decomposition of Ni/Al-LDHs has been proposed [26,27]. The presence of three different phases, in relative amounts depending on the calcination temperature, was suggested: (i) a NiO phase, containing small amounts of Al^{3+} ions; (ii) an alumina-type phase, doped with small amounts of Ni^{2+} ions which for example can be selectively removed by NaOH leachings; (iii) a spinel-type phase, on samples calcined at $T > 1000$ K. From the XRD pattern of NiAl2.98 calcined at 723 K, the alumina phase was not revealed, although the presence of a poorly crystallized Al-phase, not XRD detectable, could not be ruled out.

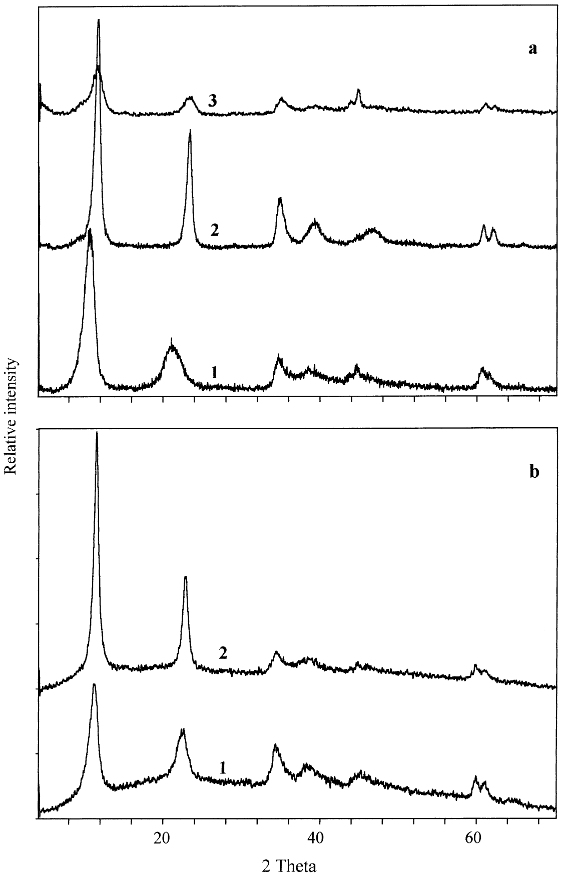

Fig. 3. XRD spectra of MgAl2.89 (Section a) and MgGa3.61 (Section b). A.p. samples, (curves 1); after calcination at 723 K and subsequent rehydroxylation at RT, (curves 2); after 5 catalytic runs, (curve 3).

3.1.3. Mg-containing rehydroxylated samples

The mixed oxides obtained by calcination of both Mg/Al and Mg/Ga LDHs could be easily rehydroxylated performing treatments during 1 h at RT into decarbonated water. Indeed the complete reconstruction under the OH^- meixnerite-like form is obtained, benefiting of the so-called memory effect [18] (Fig. 3).

A marked increase of the crystallinity could be observed comparing the XRD patterns of the a.p. and of the rehydroxylated samples. Furthermore, we noted a decrease of the interlayer distances, related to the different nature of the compensating anions, since nitrates were present in the a.p. samples, while carbonates prevailed on the rehydroxylated ones. The OH^- anions of the meixnerite-like form are indeed readily exchanged with $CO_3{}^{2-}$ when the samples are contacted with the ambient atmosphere, during the XRD experiment. This drawback is generally avoided keeping the samples under inert atmosphere.

3.1.4. Ni-containing rehydroxylated samples

Several attempts were made in order to restore under the meixnerite-like form the Ni-containing mixed oxides, since, differently from the Mg-ones, their rehydroxylation into the lamellar structure hardly occurs [20,28]. On NiAl2.98 sample calcined at 723 K, XRD analysis showed that rehydroxylation in water at 298–373 K under atmospheric pressure did not lead to the reconstruction (Table 2). The phenomenon is

Table 2
Rehydroxylation conditions of LDH samples

Sample	Calcination *T* (K)	Rehydroxylation condition				Reconstruction degree (%)[a]	Conversion (%)[b]
		medium	*T* (K)	*t* (h)	*p* (Pa)		
MgAl2.69	723	H_2O	298	1	10^5	100	19.0
MgAl2.89	723	H_2O	298	1	10^5	100	13.8
MgGa3.61	723	H_2O	298	1	10^5	100	16.5
MgGa4.53	723	H_2O	298	1	10^5	100	18.8
MgGa4.53	823	H_2O	298	1	10^5	100	19.7
MgGa6.94	723	H_2O	298	1	10^5	100	15.1
NiAl2.98	723	H_2O	298 or 373	72	10^5	0	0.1
NiAl2.98	723	H_2O	388	72	2×10^5	15	0.5
NiAl2.98	723	H_2O	433	120	6×10^5	23	0.8
NiAl2.98	723	NH_4OH[c]	433	120	6×10^5	25	7.7
NiAl2.98	633	H_2O	433	120	6×10^5	80	2.5
NiAl2.98	633	NH_4OH[c]	433	120	6×10^5	>80	6.5
NiAl2.98	673	H_2O	433	120	6×10^5	60	9
NiAl2.98	673	NH_4OH[c]	433	120	6×10^5	70	15

[a] Evaluated on the basis of the integrated intensity of the (0 0 3) reflection in the XRD patterns.

[b] After 4 h of reaction at 273 K.

[c] Aqueous solution NH_3/H_2O 0.3 wt.%.

not kinetically limited since no change occurred after 72 h of treatment. Therefore, hydrothermal treatments were performed, at higher temperature and pressure. A reconstruction degree of 23% in comparison with the a.p. sample was indeed reached for NiAl2.98 performing the s.r.t. under water (Fig. 4). The reconstruction degree was calculated on the basis of the integrated areas of the (0 0 3) XRD reflections of the LDHs.

Since the reconstruction degree remained low, it was tried to lower the precalcination temperature, in order to obtain more reversible mixed oxide structures. Indeed, 80% reconstruction was reached performing the s.r.t. under water on samples precalcined at 633 K (Fig. 4 curve 4). However TG analysis evidenced that consistent amounts of CO_3^{2-} in the range of 0.5–1 wt.%, still remained in the structure, which are able to poison the stronger basic sites. It must be recalled that the main goal of these experiments was to obtain the meixnerite-like form. This implies not only to restore the lamellar structure, but also to totally exchange the NO_3^- and CO_3^{2-} anions by OH^-, which are the active species for the targeted catalytic application. Anyway, one of the main difficulty arises from the higher affinity of these structures toward the CO_3^{2-} compensating anions [14]. Therefore, the calcination temperature of the LDH, leading to the mixed oxide, appears as a key parameter able

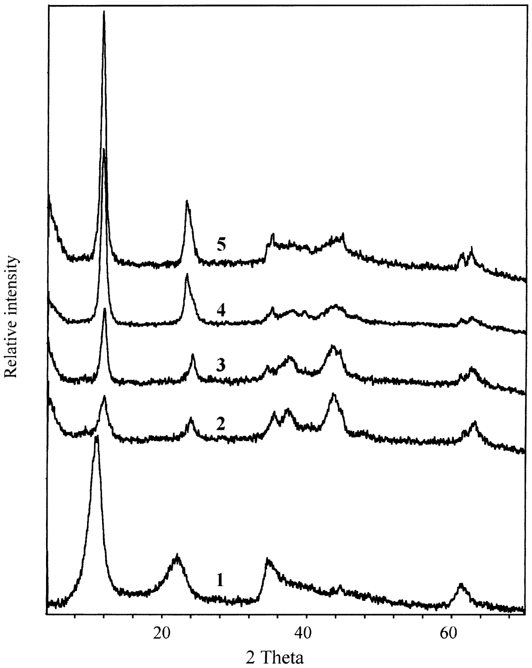

Fig. 4. XRD spectra of NiAl2.98 at different rehydroxylation degrees. A.p. samples, (curve 1); calcined at 723 K and submitted to the s.r.t. under H_2O, (curve 2); or under NH_4OH, (curve 3); calcined at 633 K and submitted to the s.r.t. under H_2O, (curve 4); or under NH_4OH, (curve 5).

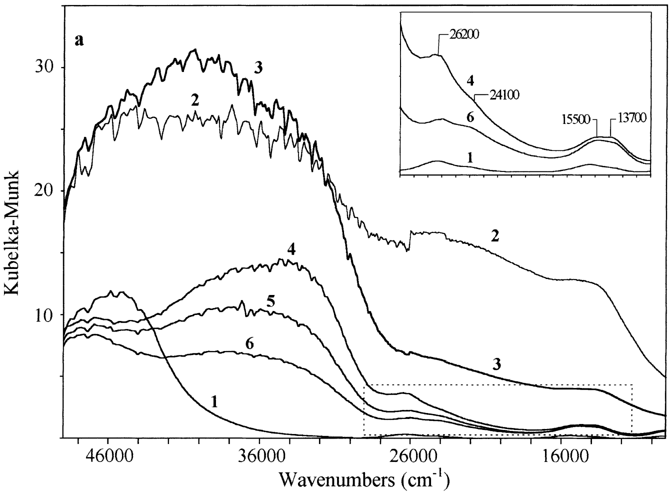

Fig. 5. UV–VIS DRS spectra of NiAl2.98. A.p. samples, (curve 1); calcined at 633 K, (curve 2); or at 723 K, (curve 3); calcined at 723 K and submitted to the s.r.t. under H_2O, (curve 4); or under NH_4OH, (curve 5); calcined at 633 K and submitted to the s.r.t. under NH_4OH, (curve 6).

to determine a good compromise between the reconstruction degree of the mixed oxides and the anionic content of the meixnerite-like compounds. According to these requirements, a different route was explored in order to increase the reconstruction degree while maintaining the calcination temperature above 633 K. The s.r.t. were then performed in an aqueous solution containing 0.5–1 wt.% of NH_4OH. An improvement of the reconstruction degree was observed, whatever the precalcination temperature (Fig. 4 curves 3, 5). In the alkaline medium, higher amounts of OH^- species were thus available for the regeneration of the Ni(Al)O mixed oxide into the meixnerite-like form as required from the lower electropositivity of Ni^{2+} than Mg^{2+}. It is remarkable that reconstruction reached 70% on NiAl2.98 precalcined at 673 K, i.e. at a temperature ensuring an extensive decomposition of interlayer anions, and submitted to the s.r.t.

3.2. UV–VIS DRS characterization

NiAl2.98 was characterized by means of UV–VIS DR spectroscopy in order to acquire further information on the Ni^{2+} environment. The a.p. LDH compound, of green color, showed weak bands at 15 500 and 26 200 cm^{-1}, with shoulders at 24 100 and 13 700 cm^{-1}, respectively, assigned to d–d transitions of Ni^{2+} ions with a distorted octahedral configuration, while the intense absorption at $\bar{\upsilon} > 42\,000$ cm^{-1} was due to charge-transfer transitions (Fig. 5 curve 1). After calcination at temperatures in the range 633–823 K, an intense and broad absorption in the UV region, with maxima at about 40 000 and 33 000 cm^{-1}, was related to the formation of a NiO-type phase [29–31] (Fig. 5 curves 2, 3). In addition, a broad and intense absorption extending up to 10 000 cm^{-1} was observed, whose intensity markedly decreased when the calcination temperature was increased (Fig. 5 curves 2, 3). This absorption was assigned to electronic transitions from the valence band to acceptor levels in the band gap, due to the presence of Ni^{3+} ions, as in non-stoichiometric nickel oxides [29,32]. This was confirmed by the black color of the sample [33]. The formation of Ni^{3+} ions was likely induced by an excess of oxygen in the external layers of NiO particles [34–36], due to the presence of trivalent Al^{3+} ions in the NiO lattice. Accordingly, this absorption showed higher intensity after calcination at 633 K, where the Al-doped NiO phase was more homogeneous, whereas it decreased after calcination at 723 K. This suggested the migration of a part of Al^{3+} ions outside the NiO lattice, therefore the formation of a more stoichiometric NiO phase.

The spectra of precalcined NiAl2.98 sample, submitted to rehydroxylation under different hydrothermal

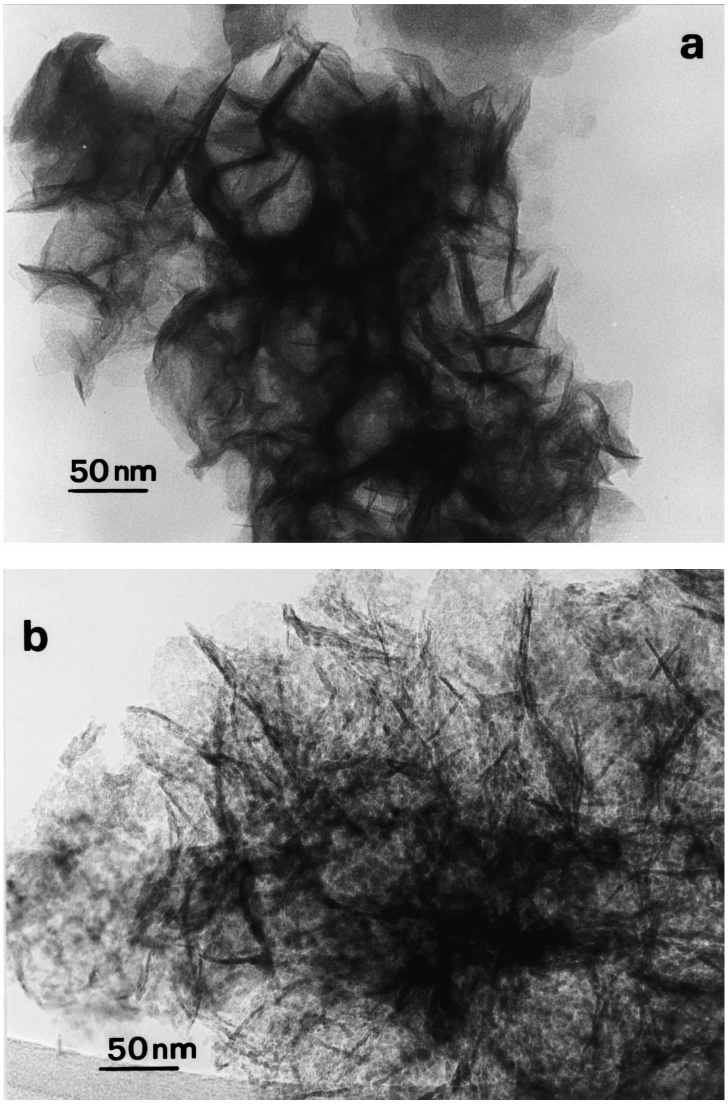

Fig. 6. TEM images of NiAl2.98 a.p. (Section a) and calcined at 673 K (Section b).

conditions, were characterized by a marked decrease of the bands at about 40 000 and 33 000 cm^{-1}, whose extent depended on the reconstruction degree of the layer structure, and by the disappearance of the broad absorption assigned to Ni^{3+} (Fig. 5 curves 4–6). Comparing the spectra of NiAl2.98 precalcined at the same temperature and submitted to the s.r.t. under water or ammonia, one can note that the decrease of NiO features was more pronounced on the latter. This finding pointed to a higher reconstruction of the LDH structure, according to the XRD results (Fig. 5 curves 4, 5). As expected, higher reconstruction degrees were obtained for NiAl2.98 calcined at lower temperature (633 K), particularly if they were rehydroxylated following the s.r.t. under ammonia (Fig. 5 curve 6).

3.3. TEM and HRTEM characterization

The morphology of NiAl2.98 sample was investigated by TEM (Fig. 6). On the a.p. sample aggregates

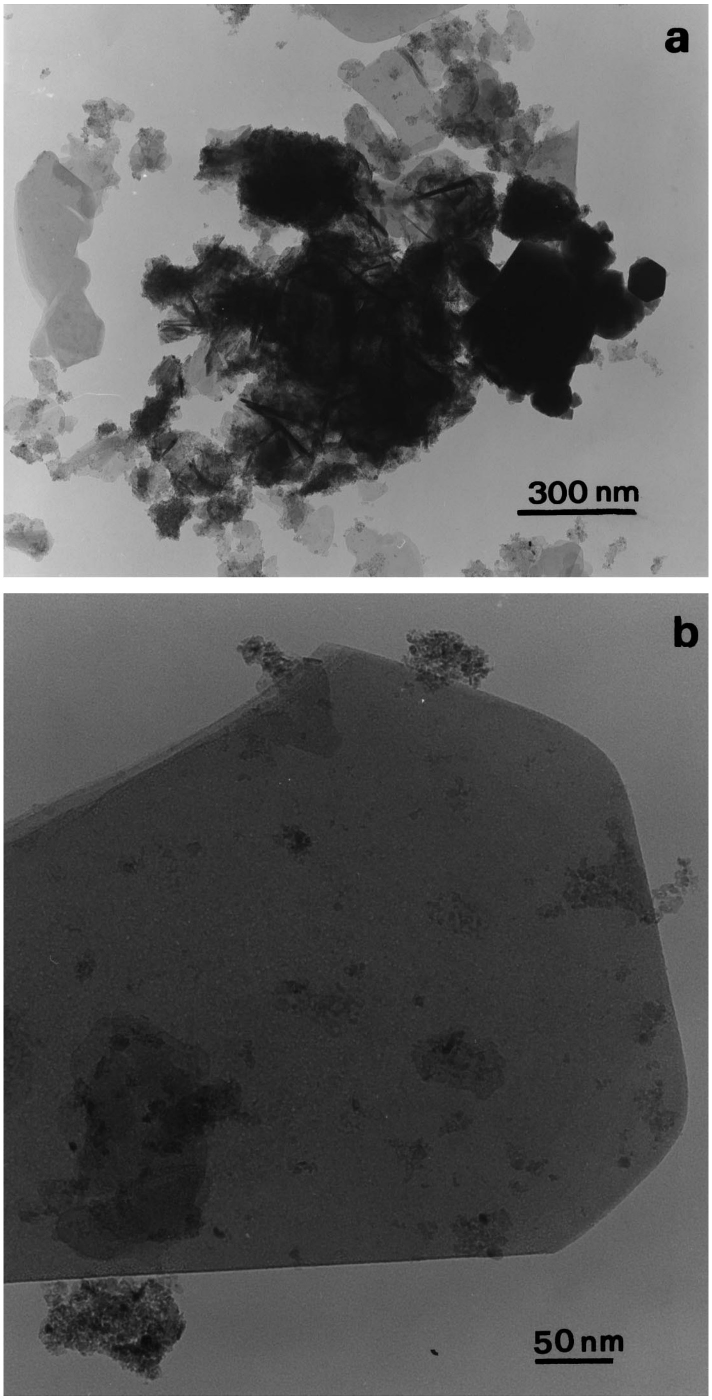

Fig. 7. TEM images of NiAl2.98 calcined at 723 K and submitted to the s.r.t. under H_2O (Sections a and b).

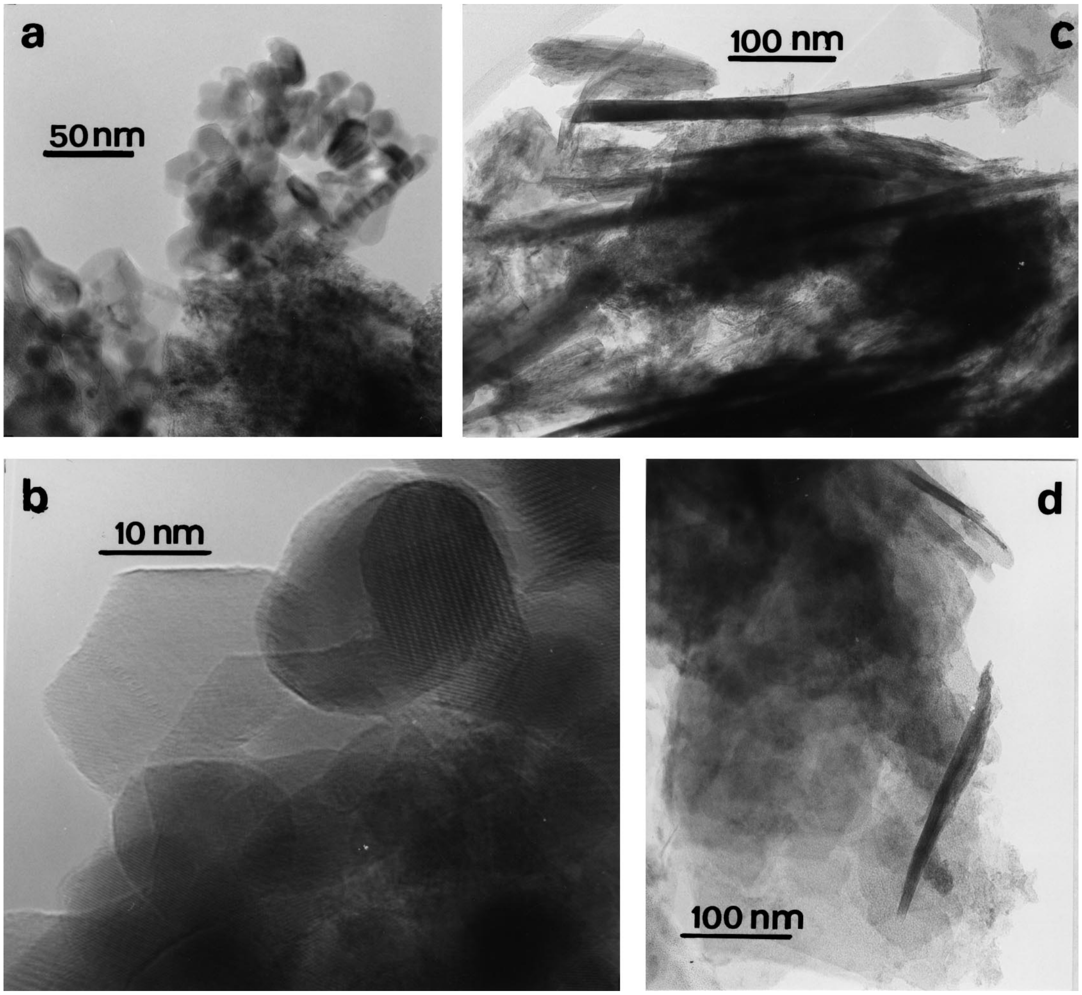

Fig. 8. TEM and HRTEM images of NiAl2.98 calcined at 633 K and submitted to the s.r.t. under H_2O (Sections a, b and c) or under NH_4OH (Section d).

of fibrous particles, characteristic of takovite compounds [25], were present (Fig. 6a). After calcination at temperatures in the range of 633–723 K (Fig. 6b), aggregates of very small crystallites were observed, anyway the general morphology of the sample was almost retained, the thermal decomposition of Ni/Al-LDHs proceeding topotactically [25], as already reported for the Mg/Al ones [28,37].

The electron micrographies of NiAl2.98 precalcined at 723 K and rehydrated in water by the s.r.t. (Fig. 7a and b) evidenced three well-distinct morphologies: (i) well crystallized particles of hexagonal shape, with regular contours and very large sizes (100–500 nm), showing no diffraction fringes, assigned to NiO, possibly Al-doped; (ii) rare aggregates of fibrous LDH particles; (iii) rounded particles of small sizes (10–20 nm). Comparatively, on this sample precalcined at 633 K and rehydroxylated under the same conditions (Fig. 8a, b and c) one can note that: (i) aggregates of NiO particles with more irregular shape and very small sizes (<20 nm) were present; (ii) the relative amount of aggregates of LDH particles was considerably higher, in agreement with the improvement of the reconstruction degree evidenced by XRD analysis; (iii) rounded particles were present in very low relative amounts. On these

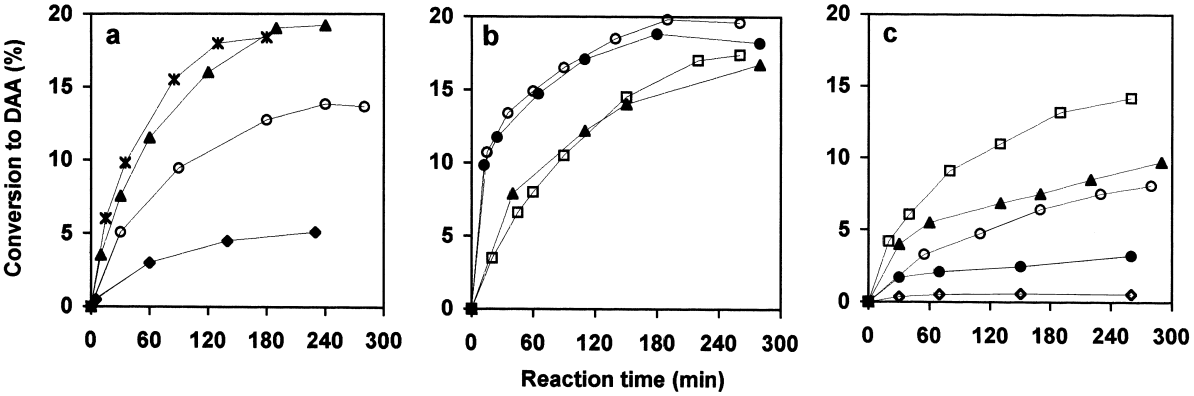

Fig. 9. Catalytic activity of Mg/Al (Section a), Mg/Ga (Section b) and Ni/Al (Section c) samples in the aldol condensation of acetone: DAA conversion as a function of reaction time. Section a: MgAl2.89 calcined at 723 K, (◆); MgAl2.89, (○); MgAl2.69, (△) calcined at 723 K and rehydroxylated at RT; NaOH, (*). Section b: MgGa6.94, (△); MgGa4.53, (●); MgGa3.61, (☐) calcined at 723 K and rehydroxylated at RT; MgGa4.53 (○) calcined at 823 K and rehydroxylated at RT. Section c: NiAl2.98 calcined at 723 K and submitted to the s.r.t. under H_2O, (◇); or under NH_4OH (△); calcined at 633 K and submitted to the s.r.t. under H_2O, (●); or under NH_4OH, (○); calcined at 673 K and submitted to the s.r.t. under NH_4OH, (☐).

latter, the distances of 0.431 and 0.320 nm between diffraction fringes allowed to identify the (1 1 0) and (1 1 1) planes, respectively, of aluminium hydroxide (JCPDS file n. 20-11) (Fig. 8b). $Al(OH)_3$ arose from the rehydroxylation of an alumina phase, possibly Ni-doped, formed during calcination, although on the calcined material it was not evidenced by TEM. The segregation of aluminum-rich phases justifies the scarce reversibility toward the lamellar structure of the Ni-based mixed oxides formed upon calcination [25–27].

The electron micrographies of precalcined NiAl2.98, rehydroxylated under ammonia atmosphere, were next examined. $Al(OH)_3$ particles were no more present on the sample precalcined at 633 K (Fig. 8d) due to their easy dissolution in alkaline solutions. Aggregates of very irregular NiO particles, with highly eroded contours were found resulting from the very high solubility of NiO and $Ni(OH)_2$ in ammonia solutions [33] in contrast with their negligible solubility in other alkaline solutions. Therefore, both Al^{3+} from $Al(OH)_3$ and Ni^{2+} from NiO dissolutions became available in the alkaline solution during the hydrothermal treatment. This could account for the precipitation of a new Ni/Al LDH phase, appearing on TEM images as small dark plots of 1–2 nm in size, completely covering the surface of the NiO particles (Fig. 8d).

3.4. Catalytic activity

All the a.p. samples, tested without pretreatment, were inactive in the acetone condensation reaction. Therefore, the layered structures containing nitrates or carbonates as compensating anions are poorly effective basic catalysts. In contrast, a catalytic activity reaching 5% conversion into DAA after 4 h of reaction was observed for the mixed oxides obtained after calcination at 723 K of the Mg-containing LDHs (Fig. 9a). However, the activities were very low in comparison to that of the same samples calcined at 723 K and totally rehydroxylated. These meixnerite-like structures were able indeed to reach a conversion into DAA comparable to that of NaOH in homogeneous phase, for example, as shown for MgAl2.69 (Fig. 9a). The amount of NaOH was chosen in order to have theoretically the same number of OH^- than in the totally exchanged LDH compound. As reported in Section 2.2, the water used for the rehydroxylation of the calcined LDHs in the activation procedure was removed by washing in acetone. It has been checked that some acetone conversion occurred only during the last washing step, anyway not exceeding 6%, due to the short contact time.

Comparing the activities of MgAl2.89 and MgAl2.69 meixnerite-like catalysts one can note that conversion steps of 13 and 18% into DAA were reached, respectively, after 4 h of reaction. Therefore,

Table 3
Acid–base characterization of the LDH samples calcined at 723 K

Sample	SS ($m^2 g^{-1}$)	ΔH CO_2 ($KJ mol^{-1}$)	(N_b)[a]		T_{maxdes} NH_3 (K)	(N_a)[b]		N_b/N_a
			meq g^{-1}	meq $m^{-2} \times 10^3$		meq g^{-1}	meq $m^2 \times 10^3$	
MgAl2.89	219	88	0.85	3.88	523	0.23	1.05	3.7
NiAl2.98	210	69	0.49	2.33	529	0.33	1.57	1.5
MgGa3.61	160	72	0.66	4.12	503	0.07	0.44	9.4
MgGa4.53	197	72	0.74	3.75	503	0.12	0.61	6.1

[a] N_b = number of basic sites.
[b] N_a = number of acid sites.

an enhancement of about 50% of the activity results from the decrease of the Mg^{2+}/Al^{3+} ratio from 2.89 to 2.69. In contrast, previous studies [11] reported that the activity of the Mg(Al)O mixed oxides increased with the Mg^{2+}/Al^{3+} ratio for the same reaction. These behaviors could account for the different nature of the active sites involved in these two types of structures. Indeed, the number of compensating OH^- sites increases at the reverse of the Mg^{2+}/Al^{3+} ratio in the meixnerite-like form, while the basicity of the acid–base pair sites goes through a maximum with this ratio in the mixed oxides [38].

High conversion steps in the range of 16–19% into DAA were also reached after 4 h of reaction for Mg/Ga samples in the meixnerite-like form (Fig. 9b). This shows that the substitution of Al^{3+} with Ga^{3+} slightly increased the catalytic activity. As expected from the previous results, their activities also depended on the Mg^{2+}/Ga^{3+} ratio, but in a different way than for the Mg/Al samples. This could account for the different nature of the crystallographic phases in the samples reported earlier, which become here the main parameter. Indeed, the highest initial reaction rate and conversion level were shown by MgGa4.53, while MgGa3.61 and MgGa6.94, containing exceeding phases, were less active. It is worthy to note that MgGa4.53 showed the highest reaction rate among the Mg-containing samples, in spite of its high Mg^{2+}/Ga^{3+} ratio. Similar conversion levels were reached using the meixnerite-like form of this sample precalcined at 723 or 823 K whose lamellar structure were totally restored (Table 2). This showed that similar activities resulted from samples precalcined in a large range of temperature, provided that the OH^- exchanged lamellar structure was achieved.

The Ni-containing mixed oxides obtained by calcination of NiAl2.98 were quite inactive, the conversion steps hardly reaching 0.1%. These activities by far lower than those of the Mg-containing mixed oxides, exhibiting specific surface areas in the same range, accounted for differences of the acid–base properties of these catalysts. This was clearly evidenced performing TPD experiments with CO_2 and NH_3 as probe molecules (Table 3). Indeed one can note that:

1. The density ratio of acid and basic sites evidenced a large excess of the latter in the Mg-containing samples, while rather similar amounts of both sites are found in the Ni-containing one.
2. Higher heat of CO_2 adsorption, in the range of 70–90 kJ/mol, therefore high basic strength, are found in the Mg-containing samples. In contrast, in the Ni-containing one, the heat of CO_2 adsorption did not exceed 70 kJ mol^{-1}, while the temperature of maximum NH_3 desorption shifted 30 K higher, showing an enhancement of the acid strength.
3. The substitution of Al^{3+} with Ga^{3+} slightly increased the density of the basic sites in the Mg-containing mixed oxides.

From these results, it is reasonable to think that the higher catalytic activity of the Mg-containing mixed oxides for the condensation reaction of acetone accounted for their higher density of basic sites, which are probably O^{2-} surface species.

Concerning now the catalytic activity of the Ni-containing samples in the meixnerite-like form obtained following the different treatments previously described (Fig. 9c), it is worthy to note that:

1. The conversion remained still low (0.8%) when a reconstruction degree of 23% was reached, performing the s.r.t. under water.
2. The conversion reached only 2.5%, even when a reconstruction degree of 80% was obtained, if the sample was previously calcined at temperatures

below 640 K, i.e. when carbonate species are not totally decomposed. In contrast, the conversion is nearly two times higher (9%), in spite of a lower reconstruction degree (60%), when the sample was precalcined at 673 K, i.e. totally decarbonated.

3. Whatever the precalcination temperature, the hydrothermal treatment of NiAl2.98 under NH_4OH increased the reconstruction degree and therefore the catalytic activity.

These results confirm that in order to obtain an active catalyst, the calcination temperature must be carefully chosen to assure a good compromise between a complete decomposition of the interlayer anions and a high reconstruction degree of the structure. Indeed, on one hand OH^- are the active sites for this reaction, whereas the presence of $CO_3{}^{2-}$ in the structure blocks the stronger basic sites. On the other hand, a low reconstruction degree means a low density of available OH^- sites, decreasing the catalytic activity. These results also explain why similar activities levels were found for Mg- and Ni-containing samples with comparable M^{2+}/M^{3+} ratios and degrees of reconstruction into the meixnerite-like form, due to their similar densities of sites. In contrast, dramatic differences occurred between the activities of their mixed oxides, where acid–base pair sites are involved.

In line with these results we observed a net decrease of conversion, from 13 to 7% when the MgAl2.89 meixnerite-like catalyst was contacted successively five times with a fresh charge of acetone during 2 h. Indeed, the XRD patterns of the used sample showed that catalyst deactivation came from a loss of the lamellar structure, therefore from the correlated decrease of the OH^- sites. However, after several catalytic runs the catalysts acquired a pale yellow color accounting for the presence of polycondensation products. Anyway, this effect seems to be less detrimental for the catalytic activity than the partial amorphization of the lamellar structure.

4. Conclusions

Meixnerite-like structures have shown to be basic solid catalysts as efficient as NaOH for the selective condensation reaction of acetone into DAA. This was due to the high density of OH^- active sites in the interlayer region, acting as an aqueous solution of NaOH. A main result of this study was to evidence that the existence of a well-defined layered structure and of an interlayer domain, where $NO_3{}^-$ and $CO_3{}^{2-}$ were completely replaced by OH^- anions were determinant for the catalytic activity. At comparable reconstruction degree of the meixnerite-like structure, the nature of the divalent and trivalent cations involved in the brucite-like layers of the LDH was a less stringent parameter. The active meixnerite-like forms were obtained following a procedure involving firstly a calcination step of the starting LDH, thus moving to a mixed oxide, and secondly a reconstruction in water of this mixed oxide into the lamellar structure, using the so-called memory effect. This route is preferable to the direct exchange, which could hardly provide a high exchange level, particularly for $CO_3{}^{2-}$, whose selectivity is very high. In this frame one can understand why the calcination temperature becomes a key parameter of the procedure which must be carefully chosen in order, on the one hand, to decompose the anions and on the other hand, to prevent the formation of a poorly reconstructible mixed oxide. Indeed, the memory effect of the mixed oxides is lost as the calcination temperature increases due to an evolution toward a spinel-like structure. In addition Ni-containing mixed oxides were intrinsically more stable than Mg-containing ones. This drawback has been greatly reduced in this work performing hydrothermal treatments in alkaline media, leading to a partial dissolution of Ni(Al)O and of the segregated alumina, which re-precipitate to give LDH. This implies obviously that for the different types of LDHs, depending on the nature of the involved cations, dedicated treatments of reconstruction should be performed.

Acknowledgements

F. Prinetto gratefully thanks ELF-Atochem for the financial support as a post-doctoral fellow.

References

[1] G.S. Salvapati, K.V. Ramanamurty, M.J. Janardanarao, J. Mol. Catal. 54 (1989) 9.
[2] E.C. Craven, J. Appl. Chem. (1963) 71.
[3] W.T. Reichle, J. Catal. 94 (1985) 547.

[4] F. Cavani, F. Trifirò, A. Vaccari, Catal. Today 11 (1991) 173.
[5] F. Trifirò, A. Vaccari, in: G. Alberti, T. Bein (Eds.), Comprehensive Supramolecular Chemistry, vol. 7, Pergamon Press, Oxford, 1996, p. 251.
[6] A. De Roy, C. Forano, K. El-Malki, J.P. Besse, in: M.L. Occelli, H. Robson (Eds.), Synthesis of Microporous Materials, vol. 2, Van Nostrand Reinhold, New York, 1992, p. 108.
[7] G. Mascolo, O. Marino, Min. Mag. 43 (1980) 619.
[8] S. Koritnig, P. Susse, Tschermaks Min. Petr. Mitt. 22 (1975) 79.
[9] K.K. Rao, M. Gravelle, J. Sanchez Valente, F. Figueras, J. Catal. 173 (1998) 115.
[10] R. Teissier, D. Tichit, F. Figueras, J. Kervenal, French Patent 95 00094 to Atochem, 1995.
[11] D. Tichit, M. Naciri Bennani, F. Figueras, R. Tessier, J. Kervenal, Appl. Clay Sci. 13 (1998) 401.
[12] G. Zhang, H. Hattori, K. Tanabe, Appl. Catal. 36 (1988) 189.
[13] K. Tanabe, G. Zhang, H. Hattori, Appl. Catal. 48 (1989) 63.
[14] D.L. Bish, Bull. Minéral. 103 (1980) 170.
[15] E.D. Dimotakis, T.J. Pinnavaia, Inorg. Chem. 29 (1990) 2393.
[16] E. Kanazaki, K. Kinugawa, Y. Ishikawa, Chem. Phys. Lett. 226 (1994) 325.
[17] K. Chibwe, W. Jones, J. Chem. Soc. Chem. Commun. (1989) 926.
[18] K. Sato, T. Wakabayashi, M. Shimada, Ind. Eng. Chem. Prod. Res. Dev. 25 (1986) 89.
[19] F. Medina Cabello, D. Tichit, B. Coq, A. Vaccari, N.T. Dung, J. Catal. 167 (1997) 142.
[20] B. Rebours, J.B. d’Espinose de la Caillerie, O. Clause, J. Am. Chem. Soc. 116 (1994) 1707.
[21] E. López-Salinas, M. García -Sanchez, M.A. Ramón-García, I. Schifter, J. Porous Mater. 3 (1996) 169.
[22] E. López-Salinas, M. García-Sánchez, M.E. Llanos-Serrano, J. Navarrete-Bolañoz, J. Phys. Chem. B 101 (1997) 5112.
[23] K. Fuda, N. Kudo, S. Kawai, T. Matsunaga, Chem. Lett. (1993) 777.
[24] R.D. Shannon, Acta Crystallogr. A 32 (1976) 751.
[25] O. Clause, B. Rebours, E. Merlen, F. Trifirò, A. Vaccari, J. Catal. 133 (1992) 231.
[26] O. Clause, M. Goncalves Coelho, M. Gazzano, D. Matteuzzi, F. Trifirò, A. Vaccari, Appl. Clay Sci. 8 (1993) 169.
[27] F. Trifirò, A. Vaccari, O. Clause, Catal. Today 21 (1994) 185.
[28] T. Sato, H. Fujita, T. Endo, M. Shimada, A. Tnunashima, React. Solids 5 (1988) 219.
[29] K. Klier, Kinet. Catal. 3 (1962) 65.
[30] M. Houalla, F. Delannay, B. Delmon, J. Phys. Chem. 85 (1981) 1704.
[31] M. Lo Jacono, M. Schiavello, A. Cimino, J. Phys. Chem. 75 (1971) 1044.
[32] M. Lo Jacono, A. Sgamellotti, A. Cimino, Z. Phys. Chem. 70 (1970) 179.
[33] Gmelins Handbuch der Anorganischen Chemie, vol. 57, Verlag Chemie, Weinheim, 1966, pp. 429, 459.
[34] A. Bielanski, J. Deren, J. Haber, J. Sloczynski, Trans. Faraday Soc. 58 (1962) 166.
[35] A.B.P. Lever, Inorganic Electronic Spectroscopy, Elsevier, Amsterdam, 1984.
[36] D. Schmitz Du Mont, A. Lule, D. Reinen, Ber. Bunsenges. Phys. Chem. 69 (1965) 76.
[37] W.T. Reichle, S.Y. Kang, D.S. Everhardt, J. Catal. 101 (1986) 352.
[38] A. Corma, V. Fornés, F. Rey, J. Catal. 148 (1994) 205.